Anna Hergenröder, Andreas Scherrieble*, Carsten Linti, Götz T. Gresser

Bone replacement material with optimized structure, manufactured using additive printing technology

https://doi.org/10.1515/cdbme-2024-2071

Abstract: Additive manufacturing with Arburg Plastic Freeforming (APF), an extrusion-based additive manufacturing process, was used to produce biomimetic bone scaffolds for assistance of osteosynthesis made of poly-ε-caprolactone (PCL) with channel structures for the ingrowth of blood vessels.

The specific creation of defined channel structures is very important to support the ingrowth of blood vessels, which significantly supports the regeneration of natural tissue.

The tibia model used was divided into the corticalis and the spongiosa to be able to compare the realization of the different requirements of the two natural structures with the printed structures separately.

Microtome cuts of the manufactured bone scaffolds with channels were prepared for characterization with light microscopy. Compression tests were carried out on a tensile testing machine. It was found that the channels in the tibial cortex led to a slightly higher stiffness compared to those without channels due to the frame outlines. Overall, however, the stiffness of the Polycaprolactone (PCL) scaffolds was significantly lower than that of natural bone. In the spongiosa scaffolds, the stiffness with channels was lower than that without channels, but still within the physiological range, as was the model without channels. The porosity was within the required range for both scaffold types.

Keywords: additive manufacturing, Arburg Plastic Freeforming (APF), bone defect implant, resorbable, poly-ε-caprolactone (PCL).

***Corresponding author: Andreas Scherrieble** Deutsche Institute für Textil- und Faserforschung Denkendorf (DITF), Körschtalstr. 26, Denkendorf, Germany, e-mail: andreas.scherrieble@ditf.de
Anna Hergenröder: DITF, Denkendorf, Germany
Carsten Linti: DITF, Denkendorf, Germany
Götz T. Gresser: DITF, Denkendorf, Germany

1 Introduction

Over 2.2 million bone transplantations are performed worldwide every year [1]. The numbers are rising, as increasing life expectancy results in increasing problems such as osteoporosis and the associated bone fractures [15]. Bone replacement from allogeneic donor material cannot meet this demand and carries the risk of rejection reactions or the transmission of diseases [2]. The use of autografts often requires long operation times, increases the risk of infections at the donor sites, and prolongs the regeneration time. This results in a great need for alternative solutions. One option receiving increasing attention in recent years is the use of individualized tissue engineering with synthetic bone scaffolds. Chances are seen above all in the field of additive manufacturing, as such methods enable a high degree of individualization of the scaffolds. The scaffolds, which are to be inserted into a bone defect, shall mimic the extracellular matrix (ECM) until the bone has regenerated and provide the bone cells with a scaffold for ingrowth. The scaffold thus shall provide temporary stabilization and an ingrowth aid for new bone cells and blood vessels and shall be absorbed and metabolized by the body during the regeneration of the bone [3].
The aim of this study is the conceptual development of a scaffold for the assisted osteosynthesis made of Polycaprolactone (PCL) using the additive manufacturing process Arburg Plastic Freeforming (APF) with a special focus on the integration of channels to support the ingrowth of blood vessels into the implant.

2 Requirements for the bone substitute

In order to create an optimal bone scaffold for the assistance of osteosynthesis, the complex hierarchical structure of the

bone must be imitated and the composition of the bone must be assessed individually depending on the patient's general state of health, age and nutrition. General requirements are the restoration of the mechanical stability of the bone in order to assume a load-bearing function at the beginning of fracture healing and the regeneration of the interrupted blood supply. This is the only way to supply the defect region with nutrients and cellular precursors and to ensure that waste products are removed [4] so that even large bone defects can heal. In order to limit local interactions between tissue and implant, no substances that irritate the surrounding tissue may be released. The bone replacement material should support the healing processes as long as the load can be taken by the new bone tissue [2]. The surface quality of the material is also important. It must favour the colonization of cells [5]. Long bones, such as the tibia, are mainly subjected to compression forces [4]. Table 1 provides an overview of the mechanical properties of human tibia corticalis and spongiosa.

Table 1: Mechanical characteristics of the human tibia.

	Compression-modulus	**strength**	**source**
Corticalis	17,4 GPa	195 MPa	[10]
	15-20 GPa	not mentioned	[6]
Spongiosa	489 ± 331 MPa	2,2 ± 331 MPa	[7]
	1091 ± 634 MPa	5,83 ± 3,42 MPa	[13]
	4-422 MPa	not mentioned	[9]

According to Martin et al. [10], however, it is very difficult to quantify the compression modulus. Due to fluctuating factors such as mineralization and fibre orientation, it is not possible to determine an exact value, but rather an order of magnitude [10]. In addition, there is no standardized method for compression tests on bones, so the values determined vary greatly [6].

Based on Haversian canals, the 3D model selected here is intended to implement channels that can serve as a guide rail for the ingrowth of small blood vessels. These are inserted both horizontally and vertically and linked together so that, ideally, a vascular system can form in the implanted replacement material. Based on the lightweight construction principle of bone, the replacement model should consist of a compact and a spongious part. A density of around 30 - 50 % is typical for the spongiosa and of around 80 - 95 % for the corticalis [8, 14]. The density in the implant is regulated by the printing density in the APF process.

In terms of pore size, Holmes et al. [11] showed that 3D-printed scaffolds with pores of 250 µm and additional channels of 500 µm for the ingrowth of blood vessels were able to achieve cell colonization and good blood flow properties. The pores should also be interconnecting for easy growth through the implant with good mass transfer [12].

A diameter of around 500 µm should therefore be aimed for when designing the channels in this work. The channels should also be interconnected. The spongiosa should be designed in such a way that pores of different sizes between 300 and 800 µm are created.

In the complex, highly branched vascular system of the bone, the blood vessels run in a simplified manner from the periosteum transversely or horizontally into the interior of the spongiosa and the corticalis and branch off along the longitudinal axis of the long bone in the bone marrow and Haversian canals. From this it can be deduced that the entire bone model should contain both vertical and horizontal channels that allow a branched vascular system to develop. In the spongiosa model, the implementation of horizontal channels is sufficient, as the intended porous design automatically creates continuous cavities in the vertical direction. Due to the less porous design of the corticalis model, channels must be built in both the horizontal and vertical directions, which are connected to each other.

3 Materials and methods

The presented study was carried out with granular resin poly-ε-caprolactone (PCL) CAPA 6800 from Perstorp, which has a molecular weight of 80,000 g/mol, a density of 1.1 g/cm³ and a melting point of 58-60 °C, which is comparable to biocompatible and biodegradable medical grade PCLs available for implants. Degradation occurs through hydrolysis or enzymatic cleavage [4]. PCL is completely absorbed within one to two years. In contrast to polylactide (PLA) or polyglycolic acid (PGA), no acidic degradation products are formed that could lead to local tissue acidification [12].

Computer Aided Design (CAD) models were initially created using the Parametric software CREO (version 5.0.6.0) with simple cube geometries in order to work out the feasibility and implementation of the individual requirements fundamentally. These findings were transferred to a more complex geometry forming tibial scaffolds (approx. 42 x 31 x 5 mm). Both, corticalis and spongiosa scaffolds were examined, each printed with and without additional channels. The aim was to investigate whether the stiffness of the scaffolds is within a physiological range and whether the scaffolds lose stiffness due to the channels. The scaffolds were produced using APF, an extrusion-based production technology, on a Freeformer 300-3X. Due to the low heat distortion temperature of the PCL, it was not possible to print the channels with a water-soluble polymer (polyvinyl acetate)

(Armat 11, Arburg). As it fused with the PCL during printing it could not be dissolved out.

The channels of twenty scaffolds were checked for continuity and the channel diameters of a random sample (n=10) were measured by light microscope images of sections produced with a microtome (Microm HM355). Therefore, the test specimens were fixated in the microtome and were cut in 5 µm-slices layer by layer to uncover the channels.

Compression tests were carried out on a Zwick 1455 tensile/compression testing machine with a 20 kN load cell in accordance with the ASTM D 695 standard (testing the compressive strength of hard plastics). Twenty specimens were clamped between cylindrical holders with a diameter of 60 mm and axially loaded at a feed rate of 1 mm/min, respectively. This corresponds to the main loading direction of long bones, such as occurs during standing [4]. To simulate the environment after implantation of the scaffold, the specimens were stored in phosphate-buffered saline solution at 37°C for 30 min before testing.

To determine the stiffness, the compressive modulus was calculated as a slope in the linear-elastic range. The cross-sectional area of the test specimens required for the calculation was determined using CREO; in the case of the spongiosa, the factor from the theoretical and actual volume was included in the calculation.

4 Results and Outlook

The filling density of the corticalis scaffolds is within the required values at 80 %. The filling density of the spongiosa scaffolds was determined to be 39 - 50 %, which is also within the required range.

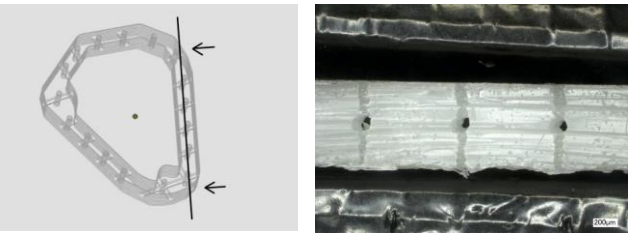

Fig. 1: left: printing model of corticalis, created with slicing software MiniMagics; black line indicates cross sectional area and arrows view direction of printed model, cut with microtome, shown on the right side.

The vertical and horizontal channels of the corticalis scaffolds were predominantly well developed with diameters between 200 and 1.000 µm (see Figure 1). However, around 6 % of the vertical channels were not continuous due to material accumulation. In order to achieve the desired diameter of the horizontal channels of 500 µm, they had to be scaled up to 1 mm in the CAD file.

Although the horizontal channels of the spongiosa scaffolds are reduced in diameter, they are still continuous. In contrast, the vertical pore pattern resulting from the polymer deposition pattern is uniform and well-defined with pore sizes between 300 – 1.000 µm.

The compression tests showed that the channels in the tibial cortex even led to a slightly higher stiffness compared to those without channels due to the reinforced edge contours (see Figure 2).

The printing of edge contours around the channels could have led to a reinforcement of the components, resulting in a slightly higher compression modulus (see Figure 3). Overall, however, the stiffness is significantly lower than that of natural bone.

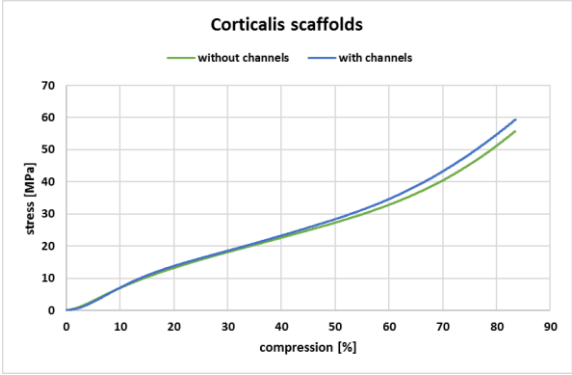

Fig. 2: Stress-compression diagram of the tibia corticalis scaffolds without / with channels (each n = 5).

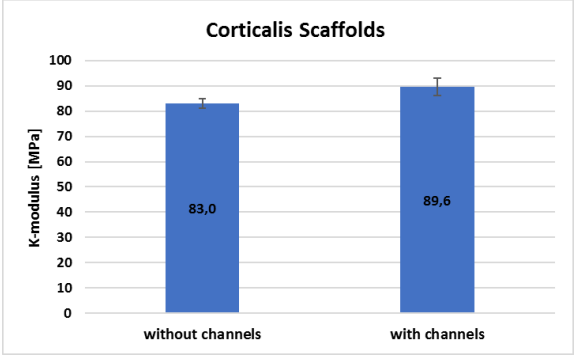

Fig. 3: Average K moduli of the tibia corticalis scaffolds without / with channels (each n = 5).

The stiffness of the spongiosa scaffolds with channels is lower than that without channels (see Figure 4 and 5). Both are still within the physiological range. The porosity achieved for both scaffold types is within the required range.

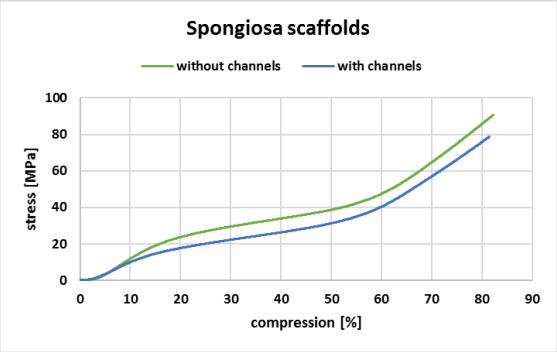

Fig. 4: Stress-compression diagram of the tibia spongiosa scaffolds without / with channels (each n = 5).

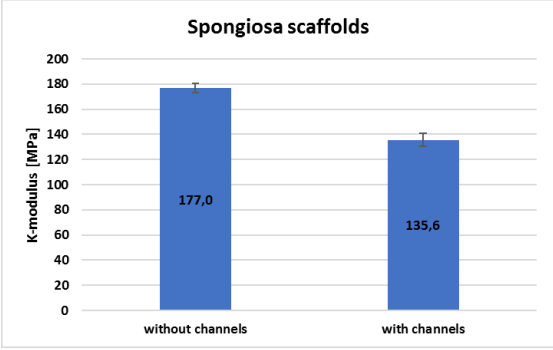

Fig. 5: Average K moduli of the tibia spongiosa scaffolds without / with channels (each n = 5).

The APF process is fundamentally suitable for the production of biomimetic scaffolds, as the requirements could be met for the most part. Overall, however, the accuracy and reproducibility seem to be limited and need to be determined in more detail by examining a greater sample size. The task of this work was to investigate the general feasibility.

The channel structures in the µm range cannot always be resolved reliably. Accuracy of printing dimensions could possibly be improved with a suitable support material. The compression stiffness of the corticalis scaffolds might be increased by HA or Tricalcium phosphate compounds or by fiber reinforcement. As channels did not significantly influence the stability, more channels could be implemented to the spongiosa scaffolds in the future.

Author Statement

Research funding: The author states no funding involved. Conflict of interest: Authors state no conflict of interest. Informed consent: Informed consent has been obtained from all individuals included in this study. Ethical approval: n.a.

References

[1] Lewandrowski, K. U.; Gresser, J. D.; Wise, D. L.; Trantol, D. J. (2000): Bioresorbable bone graft substitutes of different osteoconductivities: a histologic evaluation of osteointegration of poly(propylene glycol-co-fumaric acid)-based cement implants in rats. In: Biomaterials 21 (8), S. 757–764.

[2] Hannink, Gerjon; Arts, J. J. Chris (2011): Bioresorbability, porosity and mechanical strength of bone substitutes: what is optimal for bone regeneration? In: Injury 42 Suppl 2, S22-5.

[3] Lam, Christopher X. F.; Hutmacher, Dietmar W.; Schantz, Jan-Thorsten; Woodruff, Maria Ann; Teoh, Swee Hin (2009): Evaluation of polycaprolactone scaffold degradation for 6 months in vitro and in vivo. In: Journal of biomedical materials research. Part A 90 (3), S. 906–919.

[4] Yaszemski, M. J.; Payne, R. G.; Hayes, W. C.; Langer, R.; Mikos, A. G. (1996): Evolution of bone transplantation: molecular, cellular and tissue strategies to engineer human bone. In: Biomaterials 17 (2), S. 175–185.

[5] Freier, Thomas (2006): Biopolyesters in Tissue Engineering Applications. In: Carsten Werner (Hg.): Polymers for Regenerative Medicine. Berlin, Heidelberg: Springer Berlin Heidelberg, S. 1–61.

[6] Zhao, S.; Arnold, M.; Ma, S.; Abel, R. L.; Cobb, J. P.; Hansen, U.; Boughton, O. (2018): Standardizing compression testing for measuring the stiffness of human bone. In: Bone & joint research 7 (8), S. 524–538.

[7] Røhl, L.; Larsen, E.; Linde, F.; Odgaard, A.; Jørgensen, J. (1991): Tensile and compressive properties of cancellous bone. In: Journal of biomechanics 24 (12), S. 1143–1149.

[8] Morgan, Elise F.; Unnikrisnan, Ginu U.; Hussein, Amira I. (2018): Bone Mechanical Properties in Healthy and Diseased States. In: Annual review of biomedical engineering 20, S. 119–143.

[9] Goldstein, S. A.; Wilson, D. L.; Sonstegard, D. A.; Matthews, L. S. (1983): The mechanical properties of human tibial trabecular bone as a function of metaphyseal location. In: Journal of biomechanics 16 (12), S. 965–969.

[10] Martin, R. Bruce; Burr, David B.; Sharkey, Neil A.; Fyhrie, David P. (2015): Skeletal Tissue Mechanics. Springer New York.

[11] Holmes, Benjamin; Bulusu, Kartik; Plesniak, Michael; Zhang, Lijie Grace (2016): A synergistic approach to the design, fabrication and evaluation of 3D printed micro and nano featured scaffolds for vascularized bone tissue repair. In: Nanotechnology 27 (6), S. 64001.

[12] Bose, Susmita; Roy, Mangal; Bandyopadhyay, Amit (2012): Recent advances in bone tissue engineering scaffolds. In: Trends in biotechnology 30 (10), S. 546–554.

[13] Morgan, E. F.; Keaveny, T. M. (2001): Dependence of yield strain of human trabecular bone on anatomic site. In: Journal of biomechanics 34 (5), S. 569–577.

[14] Ott, Susan M. (2018): Cortical or Trabecular Bone: What's the Difference? In: American journal of nephrology 47 (6), S. 373–375. DOI: 10.1159/000489672.

[15] Agarwal, R.; García A.J. (2015): Biomaterial strategies for engineering implants for enhanced osseointegration and bone repair. In: Advanced drug delivery reviews 94, S. 53-62